Design, synthesis and QSAR study of certain isatin–pyridine hybrids as potential anti-proliferative agents

ARTICLE *in* EUROPEAN JOURNAL OF MEDICINAL CHEMISTRY · DECEMBER 2014

Impact Factor: 3.45 · DOI: 10.1016/j.ejmech.2014.12.010 · Source: PubMed

4 AUTHORS:

Wagdy M. Eldehna
Egyptian Russian University
13 PUBLICATIONS **25** CITATIONS
SEE PROFILE

Ayman Altoukhy
University of Pavia
1 PUBLICATION **8** CITATIONS
SEE PROFILE

Hoda Mahrous
Assistant Professor Genetic Engineering an…
20 PUBLICATIONS **84** CITATIONS
SEE PROFILE

Hatem Abdel-Aziz
National Research Center, Egypt
159 PUBLICATIONS **998** CITATIONS
SEE PROFILE

European Journal of Medicinal Chemistry 90 (2015) 684–694

Contents lists available at ScienceDirect

European Journal of Medicinal Chemistry

journal homepage: http://www.elsevier.com/locate/ejmech

Original article

Design, synthesis and QSAR study of certain isatin-pyridine hybrids as potential anti-proliferative agents

Wagdy M. Eldehna [a], Ayman Altoukhy [b], Hoda Mahrous [b], Hatem A. Abdel-Aziz [c, d, *]

[a] Department of Pharmaceutical Chemistry, Faculty of Pharmacy, Egyptian Russian University, Badr City, Cairo, P.O. Box 11829, Egypt
[b] Industrial Biotechnology Department, Genetic Engineering and Biotechnology Research Institute (GEBRI), Sadat City University, Egypt
[c] Department of Pharmaceutical Chemistry, College of Pharmacy, King Saud University, P.O. Box 2457, Riyadh 11451, Saudi Arabia
[d] Department of Applied Organic Chemistry, National Research Center, Dokki, Cairo 12622, Egypt

ARTICLE INFO

Article history:
Received 29 October 2014
Received in revised form
3 December 2014
Accepted 6 December 2014
Available online 8 December 2014

Keywords:
Isatin
Pyridine
Hybrids
Synthesis
Anti-proliferative

ABSTRACT

A hybrid pharmacophore approach was adopted to design and synthesize new series of isatin–pyridine hybrids. All the newly prepared hybrids (**5a**–**o**, **8** and **11a**–**d**) were *in vitro* evaluated for their anti-proliferative activity against three human cancer cell lines, namely HepG2 hepatocellular carcinoma, A549 lung cancer and MCF-7 breast cancer. Compound **8** emerged as the most active member against HepG2 cell line (IC_{50} = 2.5 ± 0.39 μM), with 2.7-fold increased activity than the reference drug, doxorubicin (IC_{50} = 6.9 ± 2.05 μM). Whilst, compound **11c** was found to be the most potent counterpart against A549 and MCF-7 cell lines with IC_{50} values of 10.8 ± 1.15 and 6.3 ± 0.79, respectively. The weightiness of the utilization of non-cleavable linker, as the chalcone linker, and simplification of the first group, was explored *via* the SAR study. Furthermore, a QSAR model was built to explore the structural requirements controlling the cytotoxic activities. Notably, the predicted activities by the QSAR model were very close to those experimentally observed, hinting that this model could be safely applied for prediction of more efficacious hits comprising the same skeletal framework. Finally, a theoretical kinetic study was established to predict the ADME of the active hybrids.

1. Introduction

Molecular hybridization is a valuable structural modification approach that comprises the incorporation of two or more pharmacophores into a single entity. It is based on the recognition of pharmacophoric subunits in two or more biologically active molecules with subsequent fusion of these subunits in the molecular architecture of hybrid compounds combining pre-selected characteristics of the original templates [1]. These biologically active molecules could be acting through the same mechanism of action or different mechanisms of action [2]. Moreover, the connection between the two molecular entities could be carried out using cleavable or non-cleavable linkages. Utilization of the non-cleavable linker is based on the ability of the different molecules to retain their biological activity and specific affinity for their biological targets. While, the approach using cleavable bond is based on the release of the two parental molecular structures under physiological or the enzymatic conditions that prevail at site of activity aiming to either improve poor pharmacokinetic properties or improve the activity and selectivity of the drugs and to release the two substances directly in the targeted tissues [2]. Mostly, design of the hybrid drugs aims to circumvent the drug resistance, minimize the risk of drug–drug interactions, counterbalance the known side effects associated with the other hybrid part and amplify the activity through the interaction with multiple targets as one single molecule [3,4]. In the last few years, hybrid drug design has emerged as a prime tool for the discovery of innovative anticancer therapies that can potentially overcome most of the pharmacokinetic drawbacks encountered when using conventional anticancer drugs.

Isatin (1*H*-indole-2,3-dione), **I** (Fig. 1), is a privileged scaffold and one of the most promising class of heterocyclic systems that possesses many interesting activity profiles and well-tolerated in humans [5]. BIBF1120 **II** (Fig. 1), an isatin-based triple angiokinase inhibitor disclosed by Boehringer, is currently in phase III clinical trials in non-small cell lung cancer [6]. Sunitinib, **III** (Fig. 1), trade name Sutent, is a multikinase isatin-based inhibitor targeting

* Corresponding author. Department of Pharmaceutical Chemistry, College of Pharmacy, King Saud University, P.O. Box. 2457, Riyadh 11451, Saudi Arabia.
E-mail address: hatem_741@yahoo.com (H.A. Abdel-Aziz).

http://dx.doi.org/10.1016/j.ejmech.2014.12.010
0223-5234/

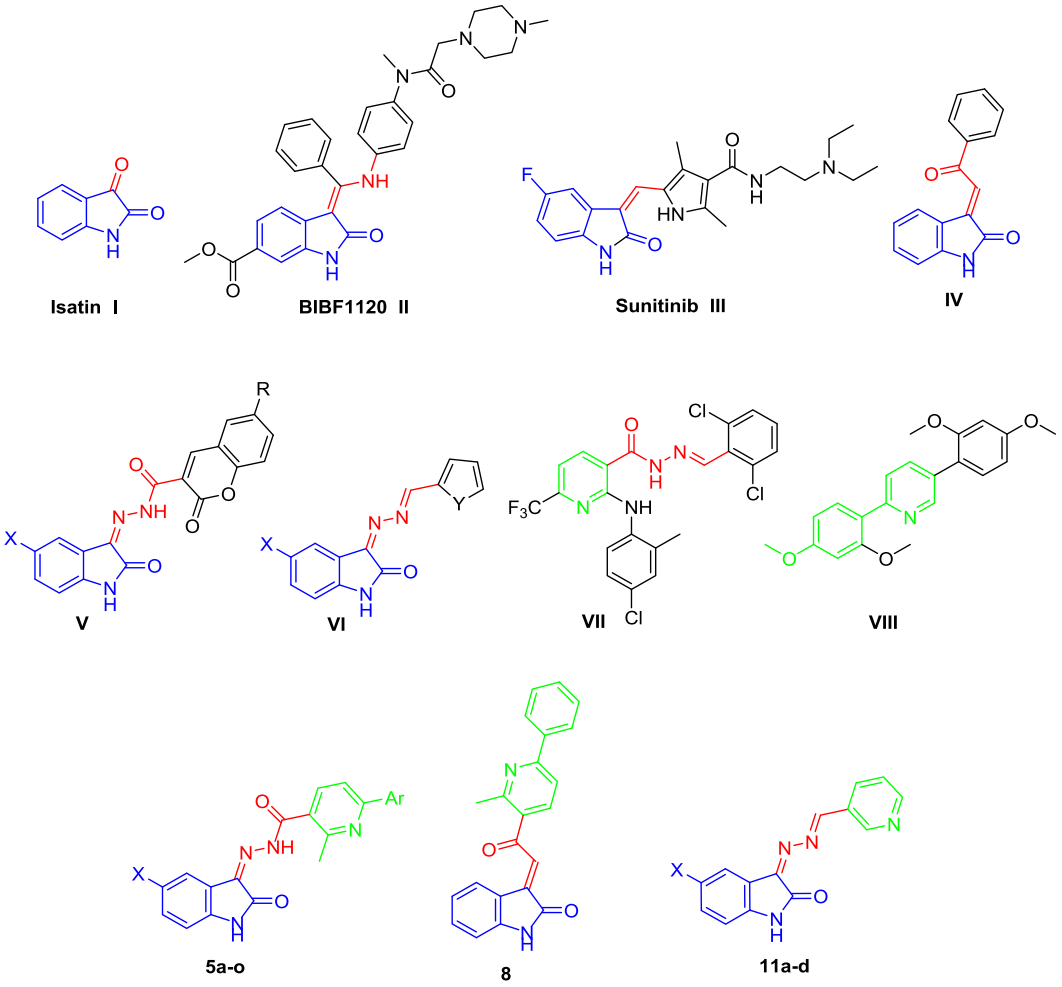

Fig. 1. Structures of compounds **I**–**VIII** and the target hybrids (**5a**–**o**, **8** and **11a**–**d**).

VEGFR-1, VEGFR-2, PDGFRβ and c-Kit. Sunitinib was approved in 2006 by the FDA for the treatment of advanced renal cell carcinoma (RCC) and gastrointestinal stromal tumors (GIST) [7–9]. The FDA approval of sunitinib paved the way to design and synthesis of various isatin-based molecules with diverse activities against cancer. In this context, many synthetic isatin-based derivatives were developed to inhibit diverse tyrosine and serine/threonine kinases, to name just a few, c-Met kinase [10], c-Src kinase [11], RET kinase [12], FLT3 kinase [13], cyclin-dependent kinases (CDKs) [14], glycogen synthase kinase 3β (GSK-3β) [15], Aurora B kinase [16], p38α MAP kinase [17], JNK3 MAP kinase [18], p90 ribosomal S6 protein kinase 2 (RSK2) [19] and Polo-like kinase 4 (PLK4) [20,21].

Over the last decade, numerous studies pointed out the importance of isatin based anticancer hybrids as promising chemotherapeutic agents. Several research groups adopted hybridization approach for the design of isatin-thiazolidine/thiazolidinone hybrid analogs as potent anti-proliferative agents [22–26]. Lee and co-workers reported two studies about the design, synthesis and cytotoxicity evaluation of two different series of isatin–benzothiazole and isatin-linked chalcones analogs against three human breast cancer cell lines. Compound **IV** (Fig. 1), elicited excellent activity with IC_{50} values of 14.99, 5.26 and 4.23 μM against MDA-MB231, MDA-MB468 and MCF7 cancer cells, respectively [27,28]. Also, A. T. Taher et al. [29] explored the anti-breast cancer activity of isatin-thiazoline and isatin-benzimidazole conjugates against breast cancer cell line MCF7. Besides, the cytotoxic activities of isatin-arylsulfoanilide [30], isatin-4-piperazinylquinoline [31], isatin-benzoxazole [32], isatin-quinazoline-4(3*H*)-one [33] and isatin-pyrazoline [34] hybrids were reported. Moreover, we reported the anticancer activity of two series of isatin-based hydrazones **V** and **VI** (Fig. 1) [35,36].

On the other hand, non-fused pyridines constitute another important class of heterocycles, which displayed interesting biological activities including anticancer activity [37–39]. Sorafenib, Regorafenib, Vismodegib and Crizotinib are examples for the clinically approved pyridine-containing anticancer drugs [40–42]. Interestingly, the pyridine-based hydrazone **VII** (Fig. 1), inhibited the growth of all tested cancer cell lines with nanomolar potency at the NCI, USA and did not show animal toxicity. Moreover, it has been selected by the Biological Evaluation Committee of NCI for testing in vivo Hollow Fiber Assay [43]. Recently, Zheng and co-workers developed a novel series of pyridine-bridged analogs of combretastatin-A4 as potential anticancer agents. Among these derivatives compound **VIII** (Fig. 1), displayed modest activities against A549 lung cancer, MDA-MB-231 breast cancer and Hela cervical cancer cell lines [44].

The present study is an extension of our ongoing efforts towards developing potent isatin-based anticancer agents [35,36,45–47], utilizing a hybrid pharmacophore approach. In view of the previous findings, we decided to design and synthesize three different set of isatin-pyridine hybrids **5a**–**o**, **8** and **11a**–**d** (Fig. 1), with the prime aim of developing potent anticancer agents. Our strategy adopted

by conjugating different 6-Arylpyridines with the isatin nucleus *via* a hydrazone (=N–NH–C=O) linkage to obtain the first group of the target compounds **5a**–**o**. Subsequently, the non-cleavable chalcone (=C–C=O) linker was selected to replace the cleavable one of the first design, affording compound **8**. Also, simplification of the first series was utilized in target hybrids **11a**–**d** to carry out further elaboration of the isatin-pyridine hybrids scaffold and to explore a valuable SAR. The latter synthesized hybrids were evaluated for their *in vitro* cytotoxic activity against three human tumor cell lines, namely, HepG2 hepatocellular carcinoma, A549 lung cancer and MCF-7 breast cancer.

2. Results and discussion

2.1. Chemistry

The synthetic pathways employed to prepare the new targeted derivatives are depicted in Schemes 1–3. In a one-pot three-component heterocyclocondensation process, ethyl 2-methyl-6-arylnicotinate **2a**–**f** was obtained *via* the reaction of enaminones **1a**–**f** with ethyl acetoacetate and ammonium acetate in refluxing acetic acid. Next, hydrazinolysis of ester derivatives **2a**–**f** was carried out through heating with excess hydrazine hydrate to furnish the hydrazide derivatives **3a**–**f**.

Preparation of the nicotinic acid hydrazones **5a**–**o** was achieved *via* the reaction of the appropriate 6-aryl-2-methylnicotinohydrazide derivative **3a**–**f** with indoline-2,3-diones **4a**–**d** in refluxed methanol in the presence of a catalytic amount of glacial acetic acid with 70–88% yield (Scheme 1).

IR spectra of the latter products showed absorption bands due to the NH groups in the region 3150-3286 cm^{-1}, in addition to a carbonyl band in the region 1670-1692 cm^{-1}. The ^1H NMR spectra of **5a**–**o** showed two singlet D_2O-exchangeable signals attributable to NH protons of the isatin and the hydrazine function (=N–NH–) in the region δ 11.27–11.44 and 13.26–13.39 ppm, respectively, while the methyl (–CH_3) protons appeared as singlet signals around δ 2.67 ppm. Furthermore, ^{13}C NMR spectra of **5a**–**o** showed signals resonating in the range δ 162.82–165.46 ppm attributable for the carbons of carbonyl groups, while the carbons of the methyl groups appeared in the range δ 23.13–25.52 ppm. Furthermore, we confirmed in a previous study the *Z*-structure of hydrazones **5a**–**o** under the basics of X-ray single crustal analysis for similar analog [46].

On the other hand, the condensation of (*E*)-3-(dimethylamino)-1-phenylprop-2-en-1-one **1a** with acetylacetone and ammonium acetate in refluxing acetic acid yielded 1-(2-Methyl-6-phenylpyridin-3-yl)ethan-1-one **6**. The later was heated with indoline-2,3-dione **4a** in ethanol in the presence of a catalytic amount of dimethylamine to give the intermediate **7** which subsequently dehydrated *via* refluxing with concentrated hydrochloric acid in glacial acetic acid to afford the compound **8** (Scheme 2).

The IR spectrum of **8** revealed the presence of two peaks at 3158 and 1690 cm^{-1} assigned to the NH and carbonyl groups, respectively. The ^1H NMR spectrum of **8** showed the singlet signal of the olefinic proton around δ 7.50 ppm, also, ^1H NMR spectrum revealed the presence of D_2O exchangable indolic NH proton at a δ 10.80 ppm. Furthermore, the ^{13}C NMR spectrum of **8** showed two signals resonating at δ 23.58 and δ 193.22 ppm attributable to the methyl ($\underline{C}H_3$) and carbonyl (=C–$\underline{C}$=O) carbons, respectively. The conformation of the exocyclic double bond of compound **8** was assigned as *E* conformation where the chemical shift of the ethylidene α-H proton appeared at δ 7.56 ppm according to the reported similar structures [48].

Finally, indoline-2,3-diones **4a**–**d** were refluxed with 99% hydrazine hydrate in methanol to obtain the corresponding hydrazone derivatives **9a**–**d**. The reaction of hydrazones **9a**–**d** with nicotinaldehyde **10** in ethanol in the presence of a catalytic amount of glacial acetic acid furnished the target derivatives **11a**–**d**.

The IR spectra of **11a**–**d** showed absorption bands around 3200 cm^{-1} for the indolic NH group in addition to the absorption bands of carbonyl groups in the region 1730–1738 cm^{-1}. ^1H NMR spectra of these compounds revealed D_2O-exchangeable signal in the region δ 10.85–11.05 ppm which were assigned to NH isatin proton, in addition to the signal of the methine proton (–CH=N–) in the region δ 8.65–8.73 ppm. Moreover, their ^{13}C NMR spectra showed signals resonating in the range δ 163.87–164.30 ppm characteristic to C=O carbons.

2.2. Biological evaluation

2.2.1. In vitro cytotoxic activity

Anti-proliferative activity of the newly synthesized isatin-pyridine hybrids **5a**–**o**, **8** and **11a**–**c** was examined in three human tumor cancer cell lines, HepG2 hepatocellular carcinoma,

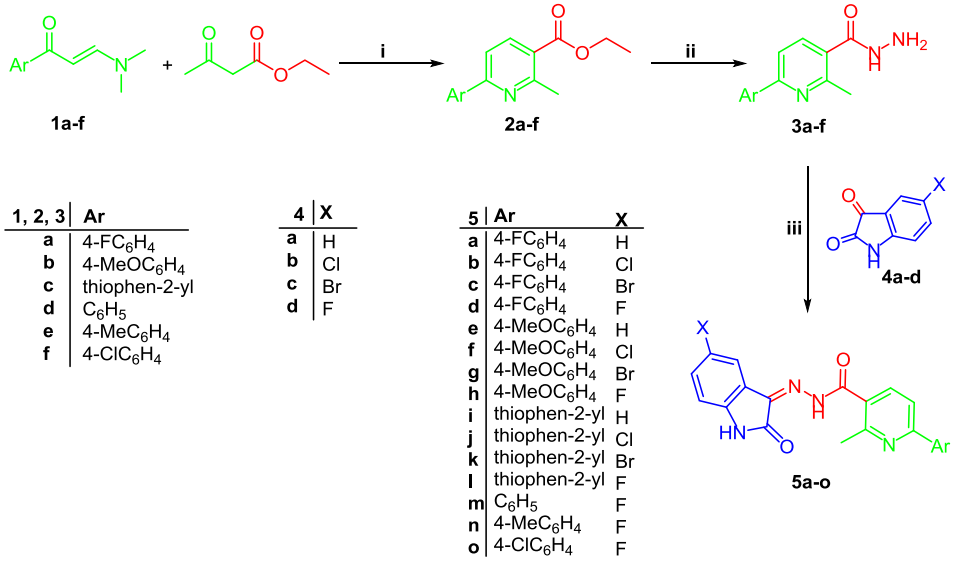

1, 2, 3	Ar
a	4-FC_6H_4
b	4-$MeOC_6H_4$
c	thiophen-2-yl
d	C_6H_5
e	4-MeC_6H_4
f	4-ClC_6H_4

4	X
a	H
b	Cl
c	Br
d	F

5	Ar	X
a	4-FC_6H_4	H
b	4-FC_6H_4	Cl
c	4-FC_6H_4	Br
d	4-FC_6H_4	F
e	4-$MeOC_6H_4$	H
f	4-$MeOC_6H_4$	Cl
g	4-$MeOC_6H_4$	Br
h	4-$MeOC_6H_4$	F
i	thiophen-2-yl	H
j	thiophen-2-yl	Cl
k	thiophen-2-yl	Br
l	thiophen-2-yl	F
m	C_6H_5	F
n	4-MeC_6H_4	F
o	4-ClC_6H_4	F

Scheme 1. Reagents and conditions: i, NH_4OAc/AcOH/reflux 5 h; ii, $NH_2NH_2.H_2O$/reflux 6 h; iii, MeOH/AcOH (catalytic)/reflux 3 h.

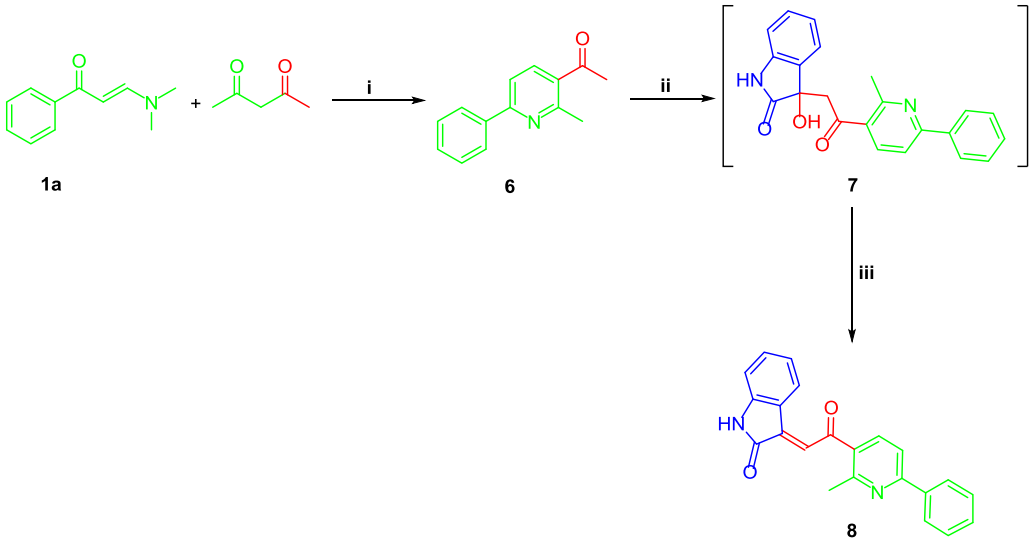

Scheme 2. Reagents and conditions: i, NH_4OAc/AcOH/reflux 3 h; ii, compound **4a**/dimethylamine/EtOH/heating at 50 °C 3 h; iii, AcOH/conc. HCl/reflux 1 h.

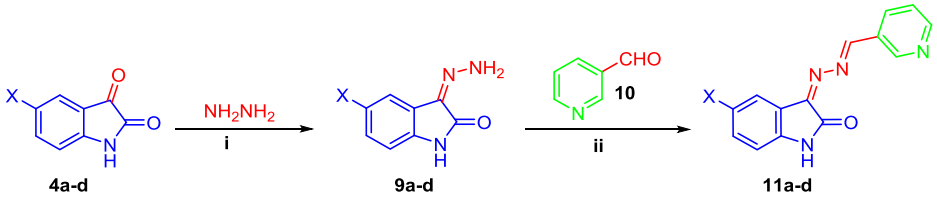

4,**9** & **11**; **a** = H, **b** = F, **c** = Cl, **d** = Br

Scheme 3. Reagents and conditions: i, MeOH/reflux 1 h; ii, EtOH/AcOH (catalytic)/reflux 4 h.

A549 lung cancer and MCF-7 breast cancer using sulforhodamine B (SRB) colorimetric assay as described by Skehan et al. [49]. Doxorubicin was included in the experiments as a reference cytotoxic compound for the three cell lines. The results were expressed as growth inhibitory concentration (IC_{50}) values which represent the compound concentrations required to produce a 50% inhibition of cell growth after 72 h of incubation compared to untreated controls (Table 1).

From the obtained results, it was obvious that several of the synthesized hybrids displayed excellent to modest growth inhibitory activity against the tested cancer cell lines. Investigations of the cytotoxic activity against HepG2 indicated that it was the most sensitive cell line to the influence of the first series hybrids and compound **8**. Compound **8** (IC_{50} = 2.5 ± 0.39 μM) was found to be the most potent derivative against HepG2 as it was 2.7 times more potent and efficacious than doxorubicin (IC_{50} = 6.9 ± 2.05 μM). Besides, compounds **11b** and **11c** with IC_{50} = 11.5 ± 1.05 and 8.7 ± 0.91 μM, respectively, showed good activity against HepG2 cancer cell line. Also, compounds **5d**, **5e**, **5f**, **5o** and **11d** were moderately active with IC_{50} values of 56.6 ± 3.30, 28.5 ± 2.03, 23.5 ± 1.57, 59.9 ± 2.47 and 59.1 ± 3.73 μM, respectively. Whilst, hybrids **5h**, **5i** and **5m** possessed weak anti-proliferative activity against HepG2 in comparison to doxorubicin (IC_{50} = 192 ± 6.91, 182 ± 4.05, and 128 ± 5.28 μM, respectively).

Concerning activity against A549, compounds **5o** and **11c** were the most active analogs through this study with IC_{50} values of 14.5 ± 0.71 and 10.8 ± 1.15, respectively. They showed 1.9- and 1.4-fold decreased potency than doxorubicin (IC_{50} = 7.6 ± 1.37 μM). Additionally, hybrids **8**, **11a** and **11b** (IC_{50} = 19.3 ± 1.34, 16.8 ± 1.92 and 19.7 ± 2.59) displayed good activity against A549 in comparison to the reference drug. On the other hand, cytotoxicity evaluation in MCF-7 cell line revealed that the first series did not elicited considerable anti-proliferative activity, whereas two members only of this series **5e** and **5f** showed weak activity with IC_{50} = 93 ± 6.41 and 71 ± 3.58 μM, respectively. Compounds **8**, **11a**, **11b** and **11d** displayed good activity with IC_{50} of 11.6 ± 0.93, 14.7 ± 2.82, 10.4 ± 1.47 and 14.9 ± 1.04 μM, respectively. Finally, compound **11c** (IC_{50} = 6.3 ± 0.79) was almost equipotent as doxorubicin (IC_{50} = 6.1 ± 1.95) and emerged as the most potent counterpart against MCF-7 in this study.

2.2.2. Structure activity relationship SAR

Based on the aforementioned biological data, many structure activity relationships could be deduced. With respect to the type of the pendant aryl group, it was found that the bioisosteric replacement of the phenyl and *p*-fluorophenyl groups with 2-thienyl group led to decrease in the activity, as compound **5l** when compared with **5d** and **5m**. Furthermore, exploration of the impact of the substitution on the 4-position of the pendant phenyl group suggested that, the order of anti-proliferative activities of the first series members is widely varied in accordance to the type of the substitution in the 5-position of isatin moiety. For the 5-fluoro substituted isatins counterparts in the first series (**5d**, **5h**, **5m**, **5n** and **5o**), the activities were decreased in the order of 4-Cl > 4-F > H > 4-OCH_3 > CH_3, hinting that grafting a lipophilic electron withdrawing substituent like halogens is more beneficial than an electron donating substituent like methyl or methoxy for the activity.

Table 1
In vitro anti-proliferative activities of the newly synthesized hybrids against HepG-2, A549 and MCF-7 cell lines.

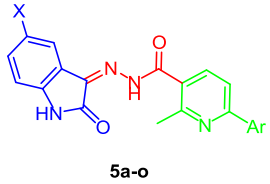

5a-o

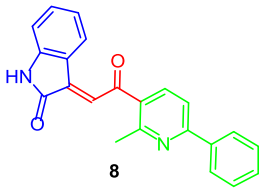

8

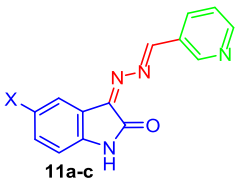

11a-c

Compound	X	Ar	IC_{50} (μM)[a]		
			HepG2	A549	MCF-7
5a	H	4-FC_6H_4	NA[b]	NA[b]	NA[b]
5b	Cl	4-FC_6H_4	NA[b]	NA[b]	NA[b]
5c	Br	4-FC_6H_4	NA[b]	NA[b]	NA[b]
5d	F	4-FC_6H_4	56.6 ± 3.30	66.6 ± 4.76	NA[b]
5e	H	4-$MeOC_6H_4$	28.5 ± 2.03	33.6 ± 2.94	93 ± 6.41
5f	Cl	4-$MeOC_6H_4$	23.5 ± 1.57	27.6 ± 1.86	71 ± 3.58
5g	Br	4-$MeOC_6H_4$	NA[b]	NA[b]	NA[b]
5h	F	4-$MeOC_6H_4$	192 ± 6.91	200 ± 12.37	NA[b]
5i	H	thiophen-2-yl	182 ± 4.05	NA[b]	NA[b]
5j	Cl	thiophen-2-yl	NA[b]	NA[b]	NA[b]
5k	Br	thiophen-2-yl	NA[b]	NA[b]	NA[b]
5l	F	thiophen-2-yl	NA[b]	NA[b]	NA[b]
5m	F	C_6H_5	128 ± 5.28	NA[b]	NA[b]
5n	F	4-MeC_6H_4	NA[b]	NA[b]	NA[b]
5o	F	4-ClC_6H_4	59.9 ± 2.47	14.5 ± 0.71	NA[b]
8	–	–	2.5 ± 0.39	19.3 ± 1.34	11.6 ± 0.93
11a	H	–	NA[b]	16.8 ± 1.92	14.7 ± 2.82
11b	F	–	11.5 ± 1.05	19.7 ± 2.59	10.4 ± 1.47
11c	Cl	–	8.7 ± 0.91	10.8 ± 1.15	6.3 ± 0.79
11d	Br	–	59.1 ± 3.73	85 ± 5.24	14.9 ± 1.04
Dox.			6.9 ± 2.05	7.6 ± 1.37	6.1 ± 1.95

[a] IC_{50} values are the mean ± S.D. of three separate experiments.
[b] NA: Compounds having IC_{50} value >200 μM.

On the other hand, replacing the cleavable hydrazone linker of the first series by the non-cleavable chalcone linker produced compound **8**, with highly improved anticancer efficacy (IC_{50}; HepG2 = 2.5 ± 0.39, A549 = 19.3 ± 1.34 and MCF-7 = 11.6 ± 0.93). This activity improvement suggested that the prepared hybrids exert their biological activity as a single entity, while the release of the two parental pharmacophoric subunits under the physiological or the enzymatic conditions sharply decreases the activity. Additionally, this improvement could be explained *via* the increased lipophilicity of the chalcone linker than the hydrazone linker.

Interestingly, simplification of the first design, hybrids **11a**–**d**, broadened and improved the activity against the three cancer cell lines. Incorporation of unsubstituted isatin moiety led to compound **11a** with good activities against the A549 and MCF-7 cell lines only. Since fluorine has a size and electronic properties similar to those of hydrogen, it is introduced as an isosteric to the hydrogen atom. Compound **11b** bears fluorine substituent at the 5-position (Alog*P* = 1.631), showed increase in the activity against the HepG2 and MCF-7 cell lines, hinting that halogens incorporation may be advantageous. Moreover, introduction of more lipophilic and bulky chlorine atom, compound **11c** (Alog*P* = 2.090), caused remarkable increase of activity against all tested tumor types. In contrast, introduction of bromine atom (more bulky than chlorine) decreased the anti-proliferative activity. Thence, the order of activities of the halogenated members in the third series, were decreased in the order of Cl > F > Br, indicating that size of the incorporated halogen is an important element for the anti-proliferative activity in this series, where, chlorine atom represents the optimal size.

2.3. 2D QSAR study

2.3.1. Development of QSAR model

QSAR analysis for anti-proliferative activity by the isatin-pyridine hybrids (**5a**–**o**, **8** and **11a**–**d**) was performed in order to correlate the biochemical data with hybrids structures, and to identify positive and negative structural features within the three hybrids designs. The analysis was run by means of the DS 2.5 software (Discovery Studio 2.5, Accelrys, Co. Ltd).

A set of the newly synthesized hybrids (**5a**–**o**, **8** and **11a**–**d**) was used as a training set with their measured pIC_{50} (the negative logarithmic value of the concentration required to produce 50% inhibition of the cancer cells) against A549 cancer cell line for QSAR modeling. "Calculate Molecular Properties" module was used for calculating the 2D molecular properties as well as energies of highest occupied and lowest unoccupied molecular orbitals (HOMO and LUMO) of the training set compounds. Different 2D descriptors such as AlogP, Finger prints, molecular properties (Molecular_-Weight), molecular property counts (Num_aromatic Rings, Num_-H_Acceptors, Num_H_Donors, Num_Rings and Num_Rotatable Bonds) and surface area and volume (Molecular_Fractional Polar Surface Area), were utilized in our model. Notably, ALogP is a measure of the hydrophobicity of the molecule that it is calculated in Discovery Studio as the Log of the octanol–water partition co-efficient using Ghose and Crippen's method [50], while Molecular_Fractional Polar Surface Area is the ratio of the polar surface area divided by the total surface area of the molecule. Multiple linear regression (MLR) protocol was employed to search for optimal QSAR models capable of correlating bioactivity variation

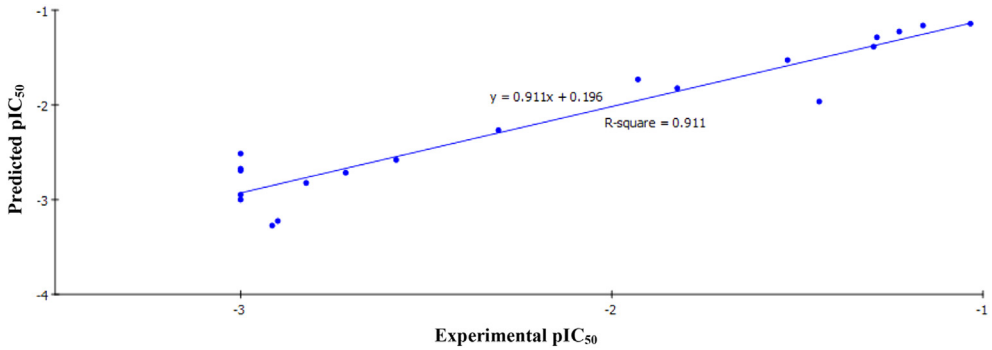

Fig. 2. Predicted versus experimental pIC_{50} of the tested compounds against A549 human cancer cell line according to Equation 1 ($r^2 = 0.911$).

across the used training set collection. QSAR model was validated employing leave one-out cross-validation by setting the folds to a number much larger than the number of samples, r2 (squared correlation coefficient value) and r2 prediction (predictive squared correlation coefficient value), residuals between the predicted and experimental activity of the test set and training set.

2.3.2. QSAR study results

Equation 1 represents the best performing QSAR model;

$$-\log IC_{50} = 352.79\ \text{ALogP} - 53.84\ \text{Molecular\_Weight} - 9.61\ \text{Num\_AromaticRings} + 3.64\ \text{Num\_H\_Donors} + 9.81\ \text{Molecular\_Fractional Polar Surface Area}. \quad (1)$$

According to Equation 1 QSAR model was represented graphically by scattering plots of the experimental versus the predicted bioactivity values $-\log IC_{50}$ for the training set compounds as shown in Fig. 2. The method used to build the model was Least-Squares, $r2 = 0.911$, r2 (adj) 1.007, r2 (pred) 0.320, Least-Squared error 0.050352, where r2 (adj) is r2 adjusted for the number of terms in the model; r2 (pred) is the prediction r2, equivalent to q2 from a leave-1-out cross-validation.

In conclusion, Equation 1 describes that the anti-proliferative activity of the synthesized hybrids against the lung A549 cancer cell line is affected by two molecular descriptors AlogP and molecular fractional polar Surface. It was found that the anti-proliferative activity is positively correlated with the increase in the hydrophobicity (ALogP) and the increase in the molecular fractional polar surface area of the synthesized compounds. This justifies the order of activity within the first and third series that mentioned in the SAR study.

2.3.3. QSAR validation

Robustness of the established QSAR model was verified by using; Leave-one-out (LOO) internal validation or cross-validation (q2), where r2 (squared correlation coefficient value) equals 0.911, r2 (pred) is equivalent to q2 from a leave-1-out cross-validation which is 0.30. In addition, validation was employed by measuring the residuals between the experimental and the predicted activities of the training set (Table 2). Interestingly, the predicted anti-proliferative activities by our QSAR model were very close to those experimentally observed, indicating that this model can be safely applied for prediction of more effective hits having the same skeletal framework.

Table 2
Experimental activity of the synthesized hybrids against the predicted activity according to Equation 1.

Compound	Experimental Activity ($-\log IC_{50}$)	Predicted Activity ($-\log IC_{50}$)	Residual
5a	−2.58092	−2.58092	0
5b	−3	−2.67477	−0.325226
5c	−2.89982	−3.22505	0.325226
5d	−1.82347	−1.82347	0
5e	−1.52634	−1.52634	0
5f	−1.44091	−1.96442	0.523507
5g	−3	−2.51469	−0.485312
5h	−2.30535	−2.26715	−0.038195
5i	−2.71684	−2.71684	0
5j	−3	−2.69383	−0.306171
5k	−2.91487	−3.27354	0.358671
5l	−3	−2.9475	−0.0525006
5m	−3	−3	0
5n	−2.82347	−2.82347	0
5o	−1.16137	−1.16137	0
8	−1.28556	−1.28556	0
11a	−1.22531	−1.22531	0
11b	−1.29447	−1.38517	0.0906959
11c	−1.03342	−1.14131	0.107889
11d	−1.92942	−1.73083	−0.198585

2.4. ADME study

The ADME of the biologically active hybrids (**5d**–**f**, **5h**, **5i**, **5m**, **5o**, **8** and **11a**–**d**) was predicted *via* a theoretical kinetic study that performed by means of Discovery Studio software (Table 3). Both, AlogP98 and PSA_2D descriptors were calculated to evaluate the lipophilicity and polar surface area. Also, solubility, absorption and CYP2D inhibition levels were predicted. Active members of the first series and compound **8** were expected to have low solubility, while, compounds **11a**–**d** showed good solubility levels. Whilst, all the examined derivatives were seemed to possess good absorption levels and predicted to be CYP2D non-inhibitors except compounds **5m**, **8** and **11a** which expected to inhibit CYP2D. Notably, all the hybrids passed the Lipinski's rule of five.

3. Conclusion

In an effort to develop potent anticancer agents, three different set of isatin-pyridine hybrids, **5a**–**o**, **8** and **11a**–**d**, were designed and synthesized. Anti-proliferative activity of the newly synthesized hybrids was examined in three human tumor cancer cell lines, namely, HepG2 hepatocellular carcinoma, A549 lung cancer and MCF-7 breast cancer using sulforhodamine B (SRB) colorimetric assay. Compound **8** emerged as the most active member against HepG2 cell line ($IC_{50} = 2.5 \pm 0.39$ μM), with 2.7-fold increased

Table 3
Computer aided ADME study of the active hybrids.

Compound	AlogP98[a]	PSA_2D[b]	Solubility[c]	Solubility level[d]	Absorption level[e]	CYP2D6[f]	CYP2D6 probability
5d	3.254	82.806	−5.208	2	0	0	0.435
5e	2.827	91.736	−4.503	2	0	0	0.396
5f	3.491	91.736	−5.268	2	0	0	0.386
5h	3.032	91.736	−4.868	2	0	0	0.396
5i	2.569	82.806	−4.418	2	0	0	0.405
5m	3.048	82.806	−4.851	2	0	1	0.564
5o	3.713	82.806	−5.608	2	0	0	0.386
8	3.695	58.672	−5.157	2	0	1	0.524
11a	1.425	64.018	−2.899	3	0	1	0.564
11b	1.631	64.018	−3.244	3	0	0	0.495
11c	2.090	64.018	−3.645	3	0	0	0.465
11d	2.174	64.018	−3.718	3	0	0	0.495

[a] Lipophilicity descriptor.
[b] Polar surface area.
[c] Solubility parameter.(0: −2 = optimal, −2: −4 = good, −4: −6 = low, −6: −8 = very low).
[d] Solubility level. (0 = extremely low, 1 = very low but possible, 2 = low, 3 = good, 4 = optimal).
[e] Absorption level. (0 = good, 1 = moderate, 2 = low, 3 = very low).
[f] CYP2D inhibition. (0 = non inhibitor, 1 = inhibitor).

activity than the reference drug, doxorubicin ($IC_{50} = 6.9 \pm 2.05$ μM). Also, it showed good activity against A549 and MCF-7 cell lines with IC_{50} values of 19.3 ± 1.34 and 11.6 ± 0.93 μM, respectively. Interestingly, the residual between the experimental and the predicted activity of compound **8** almost equals zero in the established QSAR model. Moreover, it passed the Lipinski's rule of five and was expected to have low solubility, good absorption level and CYP2D inhibitory activity. Whilst, compound **11c** was found to be the most potent derivative against A549 cell line with IC_{50} value of 10.8 ± 1.15 and 1.4-fold decreased potency than doxorubicin (IC_{50} = 7.6 ± 1.37 μM). Also, compound **11c** emerged as the most potent counterpart against MCF-7 in this study ($IC_{50} = 6.3 \pm 0.79$) and almost equipotent as doxorubicin (IC_{50} = 6.1 ± 1.95). The preliminary SAR study confirmed that utilization of non-cleavable linker and simplification of the first design are crucial elements for the anti-proliferative activity. QSAR model was established *via* the Discovery Studio 2.5 software in order to identify positive and negative structural features within the three hybrids designs. ALogP and the molecular fractional polar surface area descriptors displayed positive correlations with the anti-proliferative activity of the synthesized compounds.

4. Experimental

4.1. Chemistry

4.1.1. General

Melting points were measured with a Stuart melting point apparatus and were uncorrected. The NMR spectra were recorded by Varian Gemini-300BB 300 MHz FT-NMR spectrometers (Varian Inc., Palo Alto, CA). ^1H and ^{13}C spectra were run at 300 and 75 MHz, respectively, in deuterated dimethylsulphoxide (DMSO-d_6). Chemical shifts (δ_H) are reported relative to TMS as internal standard. All coupling constant (J) values are given in hertz. Chemical shifts (δ_C) are reported relative to DMSO-d_6 as internal standards. The abbreviations used are as follows: s, singlet; d, doublet; m, multiplet. IR spectra were recorded with a Bruker FT-IR spectrophotometer. Reaction courses and product mixtures were routinely monitored by thin layer chromatography (TLC) on silica gel precoated F_{254} Merck plates. Unless otherwise noted, all solvents and reagents were commercially available and used without further purification.

4.1.2. Ethyl 2-methyl-6-arylnicotinate *2a–f*

To a solution of the appropriate enaminone **1a–f** (5 mmol) in glacial acetic acid (15 mL), ethyl acetoacetate (5.5 mmol) and ammonium acetate (40 mmol) were added. The reaction mixture was heated under reflux for 5 h. After cooling and pouring into ice-water, the residue obtained was filtered and washed with petroleum ether then with water and finally crystallized from ethanol [51].

4.1.3. 6-Aryl-2-methylnicotinohydrazide *3a–f*

A mixture of the appropriate ester **2a–f** (5 mmol) and 99% hydrazine hydrate (2 mL) was refluxed for 6 h. The solid product obtained upon cooling was filtered off and recrystallized from dioxan to afford the corresponding 6-aryl-2-methylnicotinohydrazides **3a–f**, respectively [46].

*4.1.3.1. 6-(4-Fluorophenyl)-2-methylnicotinohydrazide (**3a**).* White crystals (yield 73%), m.p. 215–218 °C; IR (KBr, ν cm^{-1}): 3197, 3310 (NH, NH2) and 1664 (C=O); ^1H NMR (DMSO-d_6) δ ppm: 2.60 (s, 3H, CH_3), 4.51 (s, 2H, NH_2, D_2O exchangeable), 7.28 (t, 2H, H-3 and H-5 of 4-FC_6H_4, J = 9.0 Hz), 7.74 (d, 1H, H-4 pyridine, J = 8.1 Hz), 7.81 (d, 1H, H-5 pyridine, J = 8.1 Hz), 8.13 (t, 2H, H-2 and H-6 of 4-FC_6H_4, J = 9.0 Hz), 9.56 (s, 1H, NH, D_2O exchangeable).

*4.1.3.2. 6-(4-methoxyphenyl)-2-methylnicotinohydrazide (**3b**).* White crystals (yield 75%), m.p. 195–197 °C; IR (KBr, ν cm^{-1}): 3215, 3348 (NH, NH2) and 1661 (C=O); ^1H NMR (DMSO-d_6) δ ppm: 2.61 (s, 3H, CH_3), 3.80 (s, 3H, OCH_3), 4.52 (s, 2H, NH_2, D_2O exchangeable), 7.02 (d, 2H, H-3 and H-5 of 4-$OCH_3C_6H_4$, J = 9.0 Hz), 7.77 (d, 1H, H-4 pyridine, J = 8.1 Hz), 7.84 (d, 1H, H-5 pyridine, J = 8.1 Hz), 7.95 (d, 2H, H-2 and H-6 of 4-$OCH_3C_6H_4$, J = 9.0 Hz), 9.60 (s, 1H, NH, D_2O exchangeable).

*4.1.3.3. 2-Methyl-6-(thiophen-2-yl)nicotinohydrazide (**3c**).* White crystals (yield 70%), m.p. 173–175 °C; IR (KBr, ν cm^{-1}): 3235, 3327 (NH, NH2) and 1658 (C=O); ^1H NMR (DMSO-d_6) δ ppm: 2.53 (s, 3H, CH_3), 4.51 (s, 2H, NH_2, D_2O exchangeable), 7.15 (t, 1H, H-4 thiophene, J = 5.1 Hz), 7.65 (d, 1H, H-5 thiophene, J = 5.1 Hz), 7.69 (d, 1H, H-4 pyridine, J = 8.1 Hz), 7.76 (d, 1H, H-5 pyridine, J = 8.1 Hz), 7.82 (d, 1H, H-3 thiophene, J = 3.6 Hz), 9.58 (s, 1H, NH, D_2O exchangeable); ^{13}C NMR (DMSO-d_6) δ ppm: 22.76 ($\underline{C}H_3$), 115.43, 125.86, 128.47, 128.67, 128.93, 136.30, 143.86, 151.64, 155.62, 166.92.

4.1.4. General procedure for preparation of 2-methyl-N′-(2-oxoindolin-5-substituted-3-ylidene)-6-arylylnicotinohydrazide ***5a–o***

Indoline-2,3-dione derivative **4a–d** (2 mmol) was added to a suspension of the appropriate 6-aryl-2-methylnicotinohydrazide **3a–f** (2 mmol) in methanol (15 mL) and catalytic amount of glacial acetic acid. The reaction mixture was refluxed for 3 h. The precipitate formed was collected by filtration while hot, washed with hot ethanol, dried and crystallized from ethanol/DMF to afford compounds **5a–o** with 70–88% yield.

*4.1.4.1. 6-(4-Fluorophenyl)-2-methyl-N′-(2-oxoindolin-3-ylidene) nicotinohydrazide (**5a**).* Yellow powder (yield 75%), m.p. 298–300 °C; IR (KBr, ν cm^{-1}): 3150 (NH), 1680 (C=O) and 1584 (C=N); ^{1}H NMR (DMSO-d_6) δ ppm: 2.68 (s, 3H, CH_3), 6.93 (d, 1H, Ar–H, J = 8.4 Hz), 7.04 (t, 1H, Ar–H, J = 8.4 Hz), 7.31–7.41 (m, 4H, Ar–H),7.95 (d, 1H, H-4 pyridine, J = 7.8 Hz), 8.03 (d, 1H, H-5 pyridine, J = 7.8 Hz), 8.20–8.24 (m, 2H, Ar–H), 11.30 (s, 1H, $NH_{indolic}$, D_2O exchangeable), 13.34 (s, 1H, NH, D_2O exchangeable); ^{13}C NMR (DMSO-d_6) δ ppm: 25.52 ($\underline{C}H_3$), 111.09, 111.28, 115.46, 115.74, 115.92, 117.21, 119.64, 121.85, 122.63, 126.95, 129.10, 129.21, 131.34, 131.92, 134.19, 137.15, 142.52, 161.58, 162.68, 164.86. Anal. Calcd. for $C_{21}H_{15}FN_4O_2$: C, 67.37; H, 4.04; N, 14.97; Found C, 66.99; H, 4.22; N, 15.19.

*4.1.4.2. N′-(5-Chloro-2-oxoindolin-3-ylidene)-6-(4-fluorophenyl)-2-methylnicotinohydrazide (**5b**).* Orange powder (yield 79%), m.p. 327–329 °C; IR (KBr, ν cm^{-1}): 3199 (NH), 1675 (C=O) and 1579 (C=N); ^{1}H NMR (DMSO-d_6) δ ppm: 2.68 (s, 3H, CH_3), 6.95 (d, 1H, Ar–H, J = 8.4 Hz), 7.32–7.43 (m, 4H, Ar–H), 7.95 (d, 1H, H-4 pyridine, J = 8.1 Hz), 8.04 (d, 1H, H-5 pyridine, J = 8.1 Hz), 8.20–8.25 (m, 2H, Ar–H), 11.41 (s, 1H, $NH_{indolic}$, D_2O exchangeable), 13.26 (s, 1H, NH, D_2O exchangeable); ^{13}C NMR (DMSO-d_6) δ ppm: 24.72 ($\underline{C}H_3$), 113.25, 116.06, 116.33, 116.51, 117.73, 121.97, 127.27, 127.40, 129.71, 129.82, 131.76, 131.93, 134.72, 137.67, 141.78, 162.18, 163.06, 165.46. Anal. Calcd. for $C_{21}H_{14}ClFN_4O_2$: C, 61.70; H, 3.45; N, 13.70; Found C, 62.03; H, 3.68; N, 13.49.

*4.1.4.3. N′-(5-Bromo-2-oxoindolin-3-ylidene)-6-(4-fluorophenyl)-2-methylnicotinohydrazide (**5c**).* Yellow powder (yield 80%), m.p. 347–350 °C; IR (KBr, ν cm^{-1}): 3207 (NH), 1679 (C=O) and 1581 (C=N); ^{1}H NMR (DMSO-d_6) δ ppm: 2.68 (s, 3H, CH_3), 6.90 (d, 1H, Ar–H, J = 8.1 Hz), 7.31–7.37 (m, 3H, Ar–H), 7.53 (d, 1H, Ar–H, J = 8.1 Hz), 7.95 (d, 1H, H-4 pyridine, J = 7.8 Hz), 8.03 (d, 1H, H-5 pyridine, J = 7.8 Hz), 8.19–8.24 (m, 2H, Ar–H), 11.43 (s, 1H, $NH_{indolic}$, D_2O exchangeable), 13.26 (s, 1H, NH, D_2O exchangeable); ^{13}C NMR (DMSO-d_6) δ ppm: 23.92 ($\underline{C}H_3$), 113.13, 114.39, 115.47, 115.76, 11,743, 121.79, 122.56, 126.69, 129.14, 129.25, 131.62, 134.17, 136.18, 137.95, 141.58, 156.37, 161.45, 162.33, 164.93. Anal. Calcd. for $C_{21}H_{14}BrFN_4O_2$: C, 55.65; H, 3.11; N, 12.36; Found C, 55.97; H, 3.46; N, 11.99.

*4.1.4.4. N′-(5-fluoro-2-oxoindolin-3-ylidene)-6-(4-fluorophenyl)-2-methylnicotinohydrazide (**5d**).* Yellow powder (yield 83%), m.p. 345–348 °C; IR (KBr, ν cm^{-1}): 3234 (NH), 1678 (C=O) and 1588 (C=N); ^{1}H NMR (DMSO-d_6) δ ppm: 2.68 (s, 3H, CH_3), 6.91–6.96 (m, 1H, Ar–H), 7.19–7.37 (m, 4H, Ar–H), 7.95 (d, 1H, H-4 pyridine, J = 8.1 Hz), 8.03 (d, 1H, H-5 pyridine, J = 8.1 Hz), 8.19–8.24 (m, 2H, Ar–H), 11.43 (s, 1H, $NH_{indolic}$, D_2O exchangeable), 13.26 (s, 1H, NH, D_2O exchangeable); ^{13}C NMR (DMSO-d_6) δ ppm: 23.34 ($\underline{C}H_3$), 107.87, 112.38, 115.53, 115.67, 115.94, 117.20, 118.50, 120.89, 121.01, 126.25, 126.75, 129.17, 129.28, 134.21, 136.99, 138.82, 156.00, 156.79, 159.95, 161.64, 162.85, 164.92. Anal. Calcd. for $C_{21}H_{14}F_2N_4O_2$: C, 64.28; H, 3.60; N, 14.28; Found C, 64.52; H, 3.45; N, 14.39.

*4.1.4.5. 6-(4-Methoxyphenyl)-2-methyl-N′-(2-oxoindolin-3-ylidene) nicotinohydrazide (**5e**).* Yellow powder (yield 76%), m.p. 255–257 °C; IR (KBr, ν cm^{-1}): 3241 (NH), 1672 (C=O) and 1578 (C=N); ^{1}H NMR (DMSO-d_6) δ ppm: 2.67 (s, 3H, CH_3), 3.84 (s, 3H, OCH_3), 6.93 (d, 1H, Ar–H, J = 7.8 Hz), 7.05–7.48 (m, 5H, Ar–H), 7.90 (d, 1H, H-4 pyridine, J = 7.8 Hz), 7.98 (d, 1H, H-5 pyridine, J = 7.8 Hz), 8.11 (d, 2H, Ar–H, J = 8.4 Hz), 11.27 (s, 1H, $NH_{indolic}$, D_2O exchangeable), 13.30 (s, 1H, NH, D_2O exchangeable); ^{13}C NMR (DMSO-d_6) δ ppm: 23.67 ($\underline{C}H_3$), 55.23 (–O$\underline{C}H_3$), 111.11, 111.28, 114.10, 114.29, 116.21, 119.69, 120.52, 122.64, 122.80, 125.10, 126.05, 128.39, 130.10, 131.84, 136.37, 142.49, 156.74, 160.71, 162.72. Anal. Calcd. for $C_{22}H_{18}N_4O_3$: C, 68.38; H, 4.70; N, 14.50; Found C, 68.66; H, 4.47; N, 14.69.

*4.1.4.6. N′-(5-Chloro-2-oxoindolin-3-ylidene)-6-(4-methoxyphenyl)-2-methylnicotinohydrazide (**5f**).* Yellow powder (yield 78%), m.p. 315–317 °C; IR (KBr, ν cm^{-1}): 3271 (NH), 1692 (C=O) and 1580 (C=N); ^{1}H NMR (DMSO-d_6) δ ppm: 2.67 (s, 3H, CH_3), 3.83 (s, 3H, OCH_3), 6.94 (d, 1H, Ar–H, J = 8.4 Hz), 7.05 (d, 2H, Ar–H, J = 9.0 Hz), 7.40 (d, 2H, Ar–H, J = 8.4 Hz), 7.88 (d, 1H, H-4 pyridine, J = 8.4 Hz), 7.98 (d, 1H, H-5 pyridine, J = 8.4 Hz), 8.11 (d, 2H, Ar–H, J = 9.0 Hz), 11.42 (s, 1H, $NH_{indolic}$, D_2O exchangeable), 13.27 (s, 1H, NH, D_2O exchangeable); ^{13}C NMR (DMSO-d_6) δ ppm: 23.39 ($\underline{C}H_3$), 55.24 (–O$\underline{C}H_3$), 112.67, 112.80, 114.12, 114.26, 116.37, 120.19, 121.42, 125.76, 126.70, 126.82, 128.41 (2*C*), 130.05, 131.10, 131.28, 136.87, 141.15, 156.82, 160.72, 162.51. Anal. Calcd. for $C_{22}H_{17}ClN_4O_3$: C, 62.79; H, 4.07; N, 13.31; Found C, 63.08; H, 4.15; N, 13.23.

*4.1.4.7. N′-(5-Bromo-2-oxoindolin-3-ylidene)-6-(4-methoxyphenyl)-2-methylnicotinohydrazide (**5g**).* Yellow powder (yield 84%), m.p. 299–301 °C; IR (KBr, ν cm^{-1}): 3195 (NH), 1670 (C=O) and 1572 (C=N); ^{1}H NMR (DMSO-d_6) δ ppm: 2.67 (s, 3H, CH_3), 3.83 (s, 3H, OCH_3), 6.90 (d, 1H, Ar–H, J = 8.1 Hz), 7.05 (d, 2H, Ar–H, J = 8.7 Hz), 7.53 (d, 2H, Ar–H, J = 8.1 Hz), 7.88 (d, 1H, H-4 pyridine, J = 8.1 Hz), 7.98 (d, 1H, H-5 pyridine, J = 8.1 Hz), 8.11 (d, 2H, Ar–H, J = 8.7 Hz), 11.43 (s, 1H, $NH_{indolic}$, D_2O exchangeable), 13.28 (s, 1H, NH, D_2O exchangeable); ^{13}C NMR (DMSO-d_6) δ ppm: 23.13 ($\underline{C}H_3$), 55.10 (–O$\underline{C}H_3$), 112.96, 113.25, 113.94, 114.38, 116.57, 117.53, 121.79, 123.83, 125.71, 127.96, 128.79, 130.03, 134.05, 134.87, 141.50, 156.07, 156.59, 160.71, 162.33. Anal. Calcd. for $C_{22}H_{17}BrN_4O_3$: C, 56.79; H, 3.68; N, 12.04; Found C, 56.54; H, 3.34; N, 11.89.

*4.1.4.8. N′-(5-fluoro-2-oxoindolin-3-ylidene)-6-(4-methoxyphenyl)-2-methylnicotinohydrazide (**5h**).* Yellow powder (yield 82%), m.p. 306–308 °C; IR (KBr, ν cm^{-1}): 3267 (NH), 1690 (C=O) and 1578 (C=N); ^{1}H NMR (DMSO-d_6) δ ppm: 2.68 (s, 3H, CH_3), 3.83 (s, 3H, OCH_3), 6.93–6.97 (m, 1H, Ar–H), 7.05 (d, 2H, Ar–H, J = 8.7 Hz), 7.18–7.29 (m, 2H, Ar–H), 7.87 (d, 1H, H-4 pyridine, J = 7.8 Hz), 7.98 (d, 1H, H-5 pyridine, J = 7.8 Hz), 8.11 (d, 2H, Ar–H, J = 8.7 Hz), 11.30 (s, 1H, $NH_{indolic}$, D_2O exchangeable), 13.32 (s, 1H, NH, D_2O exchangeable); ^{13}C NMR (DMSO-d_6) δ ppm: 23.77 ($\underline{C}H_3$), 55.22 (–O$\underline{C}H_3$), 107.93, 112.35, 114.10, 114.28, 116.39, 117.57, 120.90, 121.02, 125.81, 126.29, 128.40, 130.05, 137.30, 138.73, 156.75, 159.91, 160.72, 162.84. Anal. Calcd. for $C_{22}H_{17}FN_4O_3$: C, 65.34; H, 4.24; N, 13.85; Found C, 65.08; H, 4.33; N, 13.78.

*4.1.4.9. 2-Methyl-N′-(2-oxoindolin-3-ylidene)-6-(thiophen-2-yl)nicotinohydrazide (**5i**).* Yellow powder (yield 70%), m.p. 285–287 °C; IR (KBr, ν cm^{-1}): 3171 (NH), 1678 (C=O) and 1577 (C=N); ^{1}H NMR (DMSO-d_6) δ ppm: 2.62 (s, 3H, CH_3), 6.93 (d, 1H, Ar–H, J = 7.8 Hz), 7.02–7.07 (m, 1H, Ar–H), 7.19 (t, 1H, H4-thiophene, J = 4.8 Hz), 7.36 (t, 1H, Ar–H, J = 7.8 Hz), 7.71 (d, 1H, H5-thiophene, J = 4.8 Hz), 7.87–7.92 (m, 3H, Ar–H), 7.99 (d, 1H, H-5 pyridine, J = 8.1 Hz), 11.31 (s, 1H, $NH_{indolic}$, D_2O exchangeable), 13.35 (s, 1H, NH, D_2O exchangeable); ^{13}C NMR (DMSO-d_6) δ ppm: 23.35 ($\underline{C}H_3$), 111.12, 111.31, 112.53, 116.71, 119.68, 120.92, 122.86, 126.52, 128.54, 128.74,

129.71, 130.28, 131.82, 137.16, 142.53, 143.85, 156.21, 162.73. Anal. Calcd. for $C_{19}H_{14}N_4O_2S$: C, 62.97; H, 3.89; N, 15.46; Found C, 63.21; H, 3.97; N, 15.29.

*4.1.4.10. N′-(5-Chloro-2-oxoindolin-3-ylidene)-2-methyl-6-(thiophen-2-yl)nicotinohydrazide (**5j**).* Yellow powder (yield 73%), m.p. 352–354 °C; IR (KBr, ν cm^{-1}): 3208 (NH), 1668 (C=O) and 1579 (C=N); ^{1}H NMR (DMSO-d_6) δ ppm: 2.62 (s, 3H, CH_3), 6.95 (d, 1H, Ar–H, J = 8.4 Hz), 7.19 (t, 1H, H4-thiophene, J = 5.1 Hz), 7.41 (d, 1H, Ar–H, J = 8.4 Hz), 7.71 (d, 1H, H5-thiophene, J = 5.1 Hz), 7.86–7.93 (m, 3H, Ar–H), 7.99 (d, 1H, H-5 pyridine, J = 7.8 Hz), 11.44 (s, 1H, $NH_{indolic}$, D_2O exchangeable), 13.30 (s, 1H, NH, D_2O exchangeable). Anal. Calcd. for $C_{19}H_{13}ClN_4O_2S$: C, 57.51; H, 3.30; N, 14.12; Found C, 57.67; H, 3.41; N, 13.97.

*4.1.4.11. N′-(5-Bromo-2-oxoindolin-3-ylidene)-2-methyl-6-(thiophen-2-yl)nicotinohydrazide (**5k**).* Yellow powder (yield 75%), m.p. 349–351 °C; IR (KBr, ν cm^{-1}): 3213 (NH), 1674 (C=O) and 1582 (C=N); ^{1}H NMR (DMSO-d_6) δ ppm: 2.62 (s, 3H, CH_3), 6.90 (d, 1H, Ar–H, J = 8.4 Hz), 7.19 (t, 1H, H4-thiophene, J = 5.1 Hz), 7.53 (d, 1H, Ar–H, J = 8.4 Hz), 7.71 (d, 1H, H5-thiophene, J = 5.1 Hz), 7.90–7.91 (m, 3H, Ar–H), 7.99 (d, 1H, H-5 pyridine, J = 8.1 Hz), 11.43 (s, 1H, $NH_{indolic}$, D_2O exchangeable), 13.26 (s, 1H, NH, D_2O exchangeable); ^{13}C NMR (DMSO-d_6) δ ppm: 24.22 ($\underline{C}H_3$), 113.11, 114.38, 115.79, 121.81, 122.51, 124.39, 126.21, 126.82, 128.52, 128.76, 129.83, 131.05, 134.28, 137.09, 141.56, 143.51, 156.26, 162.34. Anal. Calcd. for $C_{19}H_{13}BrN_4O_2S$: C, 51.71; H, 2.97; N, 12.70; Found C, 51.55; H, 3.12; N, 12.81.

*4.1.4.12. N′-(5-fluoro-2-oxoindolin-3-ylidene)-2-methyl-6-(thiophen-2-yl)nicotinohydrazide (**5l**).* Yellow powder (yield 72%), m.p. 305–307 °C; IR (KBr, ν cm^{-1}): 3238 (NH), 1665 (C=O) and 1580 (C=N); ^{1}H NMR (DMSO-d_6) δ ppm: 2.62 (s, 3H, CH_3), 6.92–6.97 (m, 1H, Ar–H), 7.18–7.26 (m, 2H, Ar–H), 7.72 (d, 1H, H5-thiophene, J = 5.1 Hz), 7.90–7.94 (m, 3H, Ar–H), 8.00 (d, 1H, H-5 pyridine, J = 8.7 Hz), 11.36 (s, 1H, $NH_{indolic}$, D_2O exchangeable), 13.39 (s, 1H, NH, D_2O exchangeable); ^{13}C NMR (DMSO-d_6) δ ppm: 23.53 ($\underline{C}H_3$),107.55, 112.50, 115.87, 117.72, 119.87, 126.30, 126.85, 128.60, 129.85, 136.35, 138.81, 143.54, 152.04, 156.80, 159.96, 162.89. Anal. Calcd. for $C_{19}H_{13}FN_4O_2S$: C, 59.99; H, 3.44; N, 14.73; Found C, 60.11; H, 3.30; N, 14.82.

*4.1.4.13. N′-(5-fluoro-2-oxoindolin-3-ylidene)-2-methyl-6-phenylnicotinohydrazide (**5m**).* Yellow powder (yield 84%), m.p. 309–311 °C; IR (KBr, ν cm^{-1}): 3185 (NH), 1676 (C=O) and 1581 (C=N); ^{1}H NMR (DMSO-d_6) δ ppm: 2.69 (s, 3H, CH_3), 6.92–6.96 (m, 1H, Ar–H), 7.20–7.52 (m, 5H, Ar–H), 7.96 (d, 1H, H-4 pyridine, J = 8.1 Hz), 8.04 (d, 1H, H-5 pyridine, J = 8.1 Hz), 8.14 (d, 2H, Ar–H, J = 7.5 Hz), 11.34 (s, 1H, $NH_{indolic}$, D_2O exchangeable), 13.37 (s, 1H, NH, D_2O exchangeable); ^{13}C NMR (DMSO-d_6) δ ppm: 23.88 ($\underline{C}H_3$), 108.13, 112.34, 117.34, 117.92, 118.25, 120.37, 120.61, 126.79, 126.92, 127.82, 128.73, 129.75, 137.26, 137.66, 138.79, 156.75, 159.92, 162.82. Anal. Calcd. for $C_{21}H_{15}FN_4O_2$: C, 67.37; H, 4.04; N, 14.97; Found C, 67.53; H, 4.22; N, 15.09.

*4.1.4.14. N′-(5-fluoro-2-oxoindolin-3-ylidene)-2-methyl-6-(p-tolyl)nicotinohydrazide (**5n**).* Orange powder (yield 81%), m.p. 314–316 °C; IR (KBr, ν cm^{-1}): 3286 (NH), 1670 (C=O) and 1578 (C=N); ^{1}H NMR (DMSO-d_6) δ ppm: 2.37 (s, 3H, 4–$C\underline{H}_3$–C_6H_4), 2.68 (s, 3H, CH_3), 6.92–6.96 (m, 1H, Ar–H), 7.18 (t, 2H, Ar–H, J = 9.0 Hz), 7.33 (d, 2H, Ar–H, J = 7.8 Hz), 7.90 (d, 1H, H-4 pyridine, J = 7.8 Hz), 8.00–8.07 (m, 3H, Ar–H), 11.30 (s, 1H, $NH_{indolic}$, D_2O exchangeable), 13.34 (s, 1H, NH, D_2O exchangeable); ^{13}C NMR (DMSO-d_6) δ ppm: 20.81 (4–$\underline{C}H_3$–C_6H_4), 23.35 ($\underline{C}H_3$),107.22, 112.49, 116.92, 117.58, 120.88, 121.01, 126.41, 126.78, 126.85, 129.32, 129.52, 134.89, 136.94, 138.76, 139.46, 156.98, 156.76, 159.92, 162.83. Anal. Calcd. for $C_{22}H_{17}FN_4O_2$: C, 68.03; H, 4.41; N, 14.43; Found C, 68.31; H, 4.27; N, 14.60.

*4.1.4.15. 6-(4-Chlorophenyl)-N′-(5-fluoro-2-oxoindolin-3-ylidene)-2-methylnicotinohydrazide (**5o**).* Yellow powder (yield 88%), m.p. 364–366 °C; IR (KBr, ν cm^{-1}): 3233 (NH), 1678 (C=O) and 1584 (C=N); ^{1}H NMR (DMSO-d_6) δ ppm: 2.68 (s, 3H, CH_3), 6.92–6.97 (m, 1H, Ar–H), 7.20 (t, 2H, Ar–H, J = 8.4 Hz), 7.57 (d, 2H, Ar–H, J = 8.7 Hz), 7.98 (d, 1H, H-4 pyridine, J = 8.4 Hz), 8.05 (d, 1H, H-5 pyridine, J = 8.4 Hz), 8.18 (d, 2H, Ar–H, J = 8.7 Hz), 11.34 (s, 1H, $NH_{indolic}$, D_2O exchangeable), 13.35 (s, 1H, NH, D_2O exchangeable). Anal. Calcd. for $C_{21}H_{14}ClFN_4O_2$: C, 61.70; H, 3.45; N, 13.70; Found C, 61.52; H, 3.59; N, 13.48.

*4.1.5. 1-(2-Methyl-6-phenylpyridin-3-yl)ethan-1-one **6***

To a solution of the enaminone **1a** (5 mmol) in glacial acetic acid (15 mL), acetylacetone (5.5 mmol) and ammonium acetate (40 mmol) were added. The reaction mixture was heated under reflux for 3 h. After cooling and pouring into ice-water, the residue obtained was filtered and washed with petroleum ether then with water and finally crystallized from ethanol. [52].

*4.1.6. 3-(2-(2-Methyl-6-phenylpyridin-3-yl)-2-oxoethylidene) indolin-2-one **8***

A mixture of indoline-2,3-dione **4a** (5 mmol), 1-(2-methyl-6-phenylpyridin-3-yl)ethan-1-one **6** (5 mmol), dimethylamine (5 drops) and ethanol (10 mL) was heated at 50 °C for 3 h. The reaction mixture was cooled to room temperature to give intermediate 3-hydroxy-3-(2-(2-methyl-6-phenylpyridin-3-yl)-2-oxoethyl)indolin-2-one **7**, which separated as a precipitate. The intermediate product **7** was then refluxed with a mixture of glacial acetic acid (15 mL) and concentrated hydrochloric acid (3 mL) for 1 h. The reaction mixture was cooled to room temperature. A solid product separated out which was filtered and recrystallized from ethanol/DMF to give red powder of compound **8** (overall yield 40%), m.p. 200–202 °C; IR (KBr, ν cm^{-1}): 3158 (NH), 1690 (C=O) and 1577 (C=N); ^{1}H NMR (DMSO-d_6) δ ppm: 2.80 (s, 3H, CH_3), 6.88 (d, 1H, H-7 isatin, J = 7.5 Hz), 6.95 (t, 1H, H-5 isatin, J = 7.5 Hz), 7.34 (t, 1H, H-6 isatin, J = 7.5 Hz), 7.51–7.55 (m, 3H, 3 Ar–H), 7.56 (s, 1H, –C$\underline{H}$=C), 7.97 (d, 1H, H-4 pyridine, J = 8.1 Hz), 8.07 (d, 1H, H-5 pyridine, J = 8.1 Hz), 8.16 (d, 2H, Ar–H, J = 8.1 Hz), 8.28 (d, 1H, H-4 isatin, J = 7.5 Hz), 10.80 (s, 1H, $NH_{indolic}$, D_2O exchangeable), ^{13}C NMR (DMSO-d_6) δ ppm: 23.58 ($\underline{C}H_3$), 111.24, 117.44, 119.89, 121.53, 126.84, 127.08, 127.93, 128.80, 129.08, 131.09, 133.09, 136.13, 137.47, 138.86, 145.03, 157.54, 157.68, 168.20, 193.22. Anal. Calcd. for $C_{22}H_{16}N_2O_2$: C, 77.63; H, 4.74; N, 8.23; Found C, 77.50; H, 4.89; N, 8.07.

*4.1.7. (Z)-3-Hydrazonoindolin-2-ones **9a–d***

To a stirred solution of **4a–d** (10 mmol) in methanol (20 mL), 99% hydrazine hydrate (2.5 mL, 50 mmol) was added. Stirring was continued at the refluxing temperature for 1 h. The precipitate of hydrazone was filtered, washed with methanol, dried and recrystallized from the glacial acetic acid to give compounds **9a–d** [36].

*4.1.8. General procedure for the synthesis of hydrazones **11a–d***

To a mixture of hydrazone **9a–d** (2 mmol) and nicotinaldehyde **10** (2 mmol) in ethanol (15 mL), 0.5 mL acetic acid was added. The reaction mixture was refluxed for 4 h, and then cooled to room temperature. The precipitate was filtered, dried and finally crystallized from ethanol to afford compounds **10a–d**.

*4.1.8.1. 3-((Pyridin-3-ylmethylene)hydrazono)indolin-2-one (**11a**).* Red powder (yield 57%), m.p. 230–233 °C; IR (KBr, ν cm^{-1}): 3165 (NH), 1730 (C=O) and 1608 (C=N); ^{1}H NMR (DMSO-d_6) δ ppm: 6.89 (d, 1H, Ar–H, J = 7.5 Hz), 7.00 (t, 1H, Ar–H, J = 7.5 Hz), 7.37 (t,

1H, Ar–H, J = 7.5 Hz), 7.57 (t, 1H, Ar–H, J = 7.5 Hz), 7.84 (d, 1H, Ar–H, J = 7.5 Hz), 8.35 (d, 1H, H-4 pyridine, J = 8.1 Hz), 8.65 (s, 1H, -CH=), 8.74 (d, 1H, H-6 pyridine, J = 4.8 Hz), 9.08 (s, 1H, H-2 pyridine), 10.85 (s, 1H, $NH_{indolic}$, D_2O exchangeable); ^{13}C NMR (DMSO-d_6) δ ppm: 110.75, 116.20, 122.53, 124.22, 124.33, 128.84, 129.21, 135.17, 145.13, 150.12, 150.33, 152.30, 157.40, 164.30. Anal. Calcd. for $C_{14}H_{10}N_4O$: C, 67.19; H, 4.03; N, 22.39; Found C, 67.32; H, 3.88; N, 22.47.

*4.1.8.2. 5-Fluoro-3-((pyridin-3-ylmethylene)hydrazono)indolin-2-one (**11b**).* Red powder (yield 51%), m.p. 217–219 °C; IR (KBr, ν cm^{-1}): 3230 (NH), 1733 (C=O) and 1619 (C=N); ^1H NMR (DMSO-d_6) δ ppm: 6.83–6.94 (m, 1H, Ar–H), 7.27 (t, 1H, Ar–H, J = 8.7 Hz), 7.62 (d, 2H, Ar–H, J = 7.8 Hz), 8.39 (d, 1H, H-4 pyridine, J = 7.8 Hz), 8.73 (s, 1H, –CH=), 8.76 (d, 1H, H-6 pyridine, J = 5.1 Hz), 9.10 (s, 1H, H-2 pyridine), 10.93 (s, 1H, $NH_{indolic}$, D_2O exchangeable). Anal. Calcd. for $C_{14}H_9FN_4O$: C, 62.69; H, 3.38; N, 20.89; Found C, 62.83; H, 3.51; N, 20.70.

*4.1.8.3. 5-Chloro-3-((pyridin-3-ylmethylene)hydrazono)indolin-2-one (**11c**).* Red powder (yield 60%), m.p. 220–223 °C; IR (KBr, ν cm^{-1}): 3169 (NH), 1732 (C=O) and 1617 (C=N); ^1H NMR (DMSO-d_6) δ ppm: 6.92 (d, 1H, Ar–H, J = 8.4 Hz), 7.47 (d, 1H, Ar–H, J = 8.4 Hz), 7.62 (t, 1H, Ar–H, J = 8.4 Hz), 7.81 (s, 1H, Ar–H), 8.34 (d, 1H, H-4 pyridine, J = 7.2 Hz), 8.72 (s, 1H, –CH =), 8.76 (d, 1H, H-6 pyridine, J = 4.5 Hz), 9.09 (s, 1H, H-2 pyridine), 11.05 (s, 1H, $NH_{indolic}$, D_2O exchangeable). Anal. Calcd. for $C_{14}H_9ClN_4O$: C, 59.06; H, 3.19; N, 19.68; Found C, 59.21; H, 3.05; N, 19.62.

*4.1.8.4. 5-Bromo-3-((pyridin-3-ylmethylene)hydrazono)indolin-2-one (**11d**).* Red powder (yield 65%), m.p. 232–234 °C; IR (KBr, ν cm^{-1}): 3206 (NH), 1738 (C=O) and 1613 (C=N); ^1H NMR (DMSO-d_6) δ ppm: 6.87 (d, 1H, Ar–H, J = 8.1 Hz), 7.33 (d, 1H, Ar–H, J = 8.1 Hz), 7.58 (t, 1H, Ar–H, J = 8.1 Hz), 7.93 (s, 1H, Ar–H), 8.32 (d, 1H, H-4 pyridine, J = 7.2 Hz), 8.70 (s, 1H, –CH=), 8.76 (d, 1H, H-6 pyridine, J = 4.5 Hz), 9.09 (s, 1H, H-2 pyridine), 11.03 (s, 1H, $NH_{indolic}$, D_2O exchangeable); ^{13}C NMR (DMSO-d_6) δ ppm: 112.75, 117.83, 123.46, 126.62, 129.05, 130.43, 134.84, 135.58, 138.47, 144.25, 150.16, 158.90, 162.28, 163.87. Anal. Calcd. for $C_{14}H_9BrN_4O$: C, 51.09; H, 2.76; N, 17.02; Found C, 50.93; H, 2.88; N, 17.31.

4.2. Biological evaluation

4.2.1. In vitro cytotoxic activity

HepG2 liver cancer, A549 colon cancer and MCF-7 breast cancer cell lines were obtained from the National Cancer Institute (Cairo, Egypt). HepG2 cells were grown in DMEM while A549 and MCF-7 were grown in RPMI-1640. Media were supplemented with 10% heat-inactivated FBS, 50 units/mL of penicillin and 50 g/mL of streptomycin and maintained at 37 °C in a humidified atmosphere containing 5% CO_2. The cells were maintained as a "monolayer culture" by serial subculturing. Cytotoxicity was determined using the SRB method as previously described by Skehan et al. [48]. Exponentially growing cells were collected using 0.25% trypsin-EDTA and seeded in 96-well plates at 1000–2000 cells/well in supplemented DMEM medium. After 24 h, cells were incubated for 72 h with various concentrations of the tested compounds as well as doxorubicin as the reference compound. Following 72 h of treatment, the cells were fixed with 10% trichloroacetic acid for 1 h at 4 °C. Wells were stained for 10 min at room temperature with 0.4% SRB dissolved in 1% acetic acid. The plates were air dried for 24 h, and the dye was solubilized with Tris–HCl for 5 min on a shaker at 1600 rpm. The optical density (OD) of each well was measured spectrophotometrically at 564 nm with an ELISA microplate reader (ChroMate-4300, FL, USA). The IC_{50} values were calculated according to the equation for Boltzmann sigmoidal concentration–response curve using the nonlinear regression models (Graph Pad, Prism Version 5). The results reported are means of at least three separate experiments. Significant differences were analyzed by one-way ANOVA wherein the differences were considered to be significant at $P < 0.05$.

Acknowledgments

The authors would like to extend their sincere appreciation to the Deanship of Scientific Research at King Saud University for its funding of this research through the Research Group Project no. RGP-VPP-321. Also, the authors acknowledge with thankfulness Dr. Dalia H. Soliman, Assistant Professor of Pharmaceutical Chemistry, Faculty of Pharmacy, (Girls), Al-Azhar University, Cairo, Egypt, for her kind guidance through the QSAR study.

Appendix A. Supplementary data

Supplementary data related to this article can be found at http://dx.doi.org/10.1016/j.ejmech.2014.12.010.

References

[1] C. Viegas-Junior, A. Danuello, V.D.S. Bolzani, E.J. Barreiro, C.A.M. Fraga, Molecular hybridization: a useful tool in the design of new drug prototypes, Curr. Med. Chem. 14 (2007) 1829–1852.
[2] S. Fortin, G. Bérubé, Advances in the development of hybrid anticancer drugs, Expert Opin. Drug Discov. 8 (2013) 1029–1047.
[3] B. Meunier, Hybrid molecules with a dual mode of action: dream or reality? Acc. Chem. Res. 41 (2008) 69–77.
[4] N. Hulsman, J.P. Medema, C. Bos, A. Jongejan, R. Leurs, M.J. Smit, I.J. de Esch, D. Richel, M. Wijtmans, Chemical insights in the concept of hybrid drugs: the antitumor effect of nitric oxide-donating aspirin involves a quinone methide but not nitric oxide nor aspirin, J. Med. Chem. 50 (2007) 2424–2431.
[5] M. Kidwai, A. Jahan, N.K. Mishra, Isatins: a diversity orientated biological profile, Med. Chem. 4 (2014) 451–468.
[6] G.J. Roth, A. Heckel, F. Colbatzky, S. Handschuh, J. Kley, T. Lehmann-Lintz, R. Lotz, U. Tontsch-Grunt, R. Walter, F. Hilberg, Design, synthesis, and evaluation of indolinones as triple angiokinase inhibitors and the discovery of a highly specific 6-methoxycarbonyl-substituted indolinone (BIBF 1120), J. Med. Chem. 52 (2009) 4466–4480.
[7] R. R Jr., Sunitinib: a VEGF and PDGF receptor protein kinase and angiogenesis inhibitor, Biochem. Biophys. Res. Commun. 356 (2007) 323–328.
[8] R.J. Motzer, M.D. Michaelson, B.G. Redman, G.R. Hudes, G. Wilding, R.A. Figlin, M.S. Ginsberg, S.T. Kim, C.M. Baum, S.E. DePrimo, J.Z. Li, C.L. Bello, C.P. Theuer, D.J. George, B.I. Rini, Activity of SU11248, a multitargeted inhibitor of vascular endothe-lial growth factor receptor and platelet-derived growth factor receptor, in patients with metastatic renal cell carcinoma, J. Clin. Oncol. 24 (2006) 16–24.
[9] H. Prenen, J. Cools, N. Mentens, C. Folens, R. Sciot, P. Schöffski, A.V. Oosterom, P. Marynen, M. Debiec-Rychter, Efficacy of the kinase inhibitor SU11248 against gastrointestinal stromaltumor mutants refractory to imatinib mesylate, Clin. Cancer Res. 12 (2006) 2622–2627.
[10] Z. Liang, D. Zhang, J. Ai, L. Chen, H. Wang, X. Kong, M. Zheng, H. Liu, C. Luo, M. Geng, H. Jiang, K. Chen, Identification and synthesis of N′-(2-oxoindolin-3-ylidene)hydrazide derivatives against c-Met kinase, Bioorg. Med. Chem. Lett. 21 (2011) 3749–3754.
[11] H. Guan, A.D. Laird, R.A. Blake, C. Tang, C. Liang, Design and synthesis of aminopropyl tetrahydroindole-based indolin-2-ones as selective and potent inhibitors of Src and Yes tyrosine kinase, Bioorg. Med. Chem. Lett. 14 (2004) 187–190.
[12] L. Mologni, R. Rostagno, S. Brussolo, P.P. Knowles, S. Kjaer, J. Murray-Rust, E. Rosso, A. Zambon, L. Scapozza, N.Q. McDonald, V. Lucchini, C. Gambacorti-Passerini, Synthesis, structure–activity relationship and crystallographic studies of 3-substituted indolin-2-one RET inhibitors, Bioorg. Med. Chem. 18 (2010) 1482–1496.
[13] A.D. Jagtap, P.-T. Chang, J.-R. Liu, H.-C. Wang, N.B. Kondekar, L.-J. Shen, H.-W. Tseng, G.S. Chen, J.-W. Chern, Novel acylureidoindolin-2-one derivatives as dual Aurora B/FLT3 inhibitors for the treatment of acute myeloid leukemia, Eur. J. Med. Chem. 85 (2014) 268–288.
[14] H.N. Bramson, J. Corona, S.T. Davis, S.H. Dickerson, M. Edelstein, S.V. Frye, R.T. Gampe Jr., P.A. Harris, A. Hassell, W.D. Holmes, R.N. Hunter, K.E. Lackey, B. Lovejoy, M.J. Luzzio, V. Montana, W.J. Rocque, D. Rusnak, L. Shewchuk, J.M. Veal, D.H. Walker, L.F. Kuyper, Oxindole-based inhibitors of cyclin-dependent kinase 2 (CDK2): design, synthesis, enzymatic activities, and X-ray crystallographic analysis, J. Med. Chem. 44 (2001) 4339–4358.

[15] P. Zhao, Y. Li, G. Gao, S. Wang, Y. Yan, X. Zhan, Z. Liu, Z. Mao, S. Chen, L. Wang, Design, synthesis and biological evaluation of N-alkyl or aryl substituted isoindigo derivatives as potential dual cyclin-dependent kinase 2 (CDK2)/glycogen synthase kinase 3β (GSK-3β) phosphorylation inhibitors, Eur. J. Med. Chem. 86 (2014) 165–174.

[16] H.-C. Wang, A.D. Jagtap, P.-T. Chang, J.-R. Liu, C.-P. Liu, H.-W. Tseng, G.S. Chen, J.-W. Chern, Bioisosteric replacement of an acylureido moiety attached to an indolin-2-one scaffold with a malonamido or a 2/4-pyridinoylamido moiety produces a selectively potent Aurora-B inhibitor, Eur. J. Med. Chem. 84 (2014) 312–334.

[17] P. Eastwood, J. González, E. Gómez, B. Vidal, F. Caturla, R. Roca, C. Balagué, A. Orellana, M. Domínguez, Indolin-2-one p38α inhibitors I: design, profiling and crystallographic binding mode, Bioorg. Med. Chem. Lett. 21 (2011) 4130–4133.

[18] J. Cao, H. Gao, G. Bemis, F. Salituro, M. Ledeboer, E. Harrington, S. Wilke, P. Taslimi, S. Pazhanisamy, X. Xie, M. Jacobs, J. Green, Structure-based design and parallel synthesis of *N*-benzyl isatin oximes as JNK3 MAP kinase inhibitors, Bioorg. Med. Chem. Lett. 19 (2009) 2891–2895.

[19] Y. Zhong, M. Xue, X. Zhao, J. Yuan, X. Liu, J. Huang, Z. Zhao, H. Li, Y. Xu, Substituted indolin-2-ones as p90 ribosomal S6 protein kinase 2 (RSK2) inhibitors: molecular docking simulation and structure–activity relationship analysis, Bioorg. Med. Chem. 21 (2013) 1724–1734.

[20] R. Laufer, B. Forrest, S.-W. Li, Y. Liu, P. Sampson, L. Edwards, Y. Lang, D.E. Awrey, G. Mao, O. Plotnikova, G. Leung, R. Hodgson, I. Beletskaya, J.M. Mason, X. Luo, X. Wei, Y. Yao, M. Feher, F. Ban, R. Kiarash, E. Green, T.W. Mak, G. Pan, H.W. Pauls, The discovery of PLK4 inhibitors: (*E*)-3-((1*H*-Indazol-6-yl)methylene)indolin-2-ones as novel Antiproliferative agents, J. Med. Chem. 56 (2013) 6069–6087.

[21] P.B. Sampson, Y. Liu, N.K. Patel, M. Feher, B. Forrest, S.-W. Li, L. Edwards, R. Laufer, Y. Lang, F. Ban, D.E. Awrey, G. Mao, O. Plotnikova, G. Leung, R. Hodgson, J. Mason, X. Wei, R. Kiarash, E. Green, W. Qui, N.Y. Chirgadze, T.W. Mak, G. Pan, H.W Pauls, THe discovery of Polo-like kinase 4 inhibitors: design and Optimization of Spiro[cyclopropane-1,3'[3H]indol]-2'(1'H)-ones as Orally Bioavailable antitumor agents, J. Med. Chem. Accept. Manuscr. (DOI: 10.1021/jm500537u).

[22] D. Havrylyuk, N. Kovach, B. Zimenkovsky, O. Vasylenko, R. Lesyk, Synthesis and anticancer activity of isatin-based pyrazolines and thiazolidines conjugates, Arch. Pharm. Chem. Life Sci. 344 (2011) 514–522.

[23] P.K. Ramshid, S. Jagadeeshan, A. Krishnan, M. Mathew, S.A. Nair, M.R. Pillai, Synthesis and *in vitro* evaluation of some isatin-thiazolidinone hybrid analogues as anti-proliferative agents, Med. Chem. 6 (2010) 306–312.

[24] D. Kaminskyy, D. Khyluk, O. Vasylenko, L. Zaprutko, R. Lesky, A. Facile, Synthesis and anticancer activity evaluation of Spiro[Thiazolidinone-Isatin] conjugates, Sci. Pharm. 79 (2011) 763–777.

[25] D. Havrylyuk, B. Zimenkovsky, O. Vasylenko, A. Gzella, R. Lesyk, Synthesis of new 4-Thiazolidinone-, pyrazoline-, and isatin-based conjugates with promising antitumor activity, J. Med. Chem. 55 (2012) 8630–8641.

[26] S. Wang, Y. Zhao, G. Zhang, Y. Lv, N. Zhang, P. Gong, Design, synthesis and biological evaluation of novel 4-thiazolidinones containing indolin-2-one moiety as potential antitumor agent, Eur. J. Med. Chem. 46 (2011) 3509–3518.

[27] V.R. Solomon, C. Hu, H. Lee, Hybrid pharmacophore design and synthesis of isatin–benzothiazole analogs for their anti-breast cancer activity, Bioorg. Med. Chem. 17 (2009) 7585–7592.

[28] C. Karthikeyan, V.R. Solomon, H. Lee, P. Trivedi, Design, synthesis and biological evaluation of some isatin-linked chalcones as novel anti-breast cancer agents: a molecular hybridization approach, Biomed. Prev. Nutr. 3 (2013) 325–330.

[29] A.T. Taher, N.A. Khalil, E.M. Ahmed, Synthesis of novel isatin-thiazoline and isatin-benzimidazole conjugates as anti-breast Cancer agents, Arch. Pharm. Res. 34 (2011) 1615–1621.

[30] A. Natarajan, Y. Guo, F. Harbinski, Y.-H. Fan, H. Chen, L. Luus, J. Diercks, H. Aktas, M. Chorev, J.A. Halperin, Novel arylsulfoanilide-oxindole hybrid as an anticancer agent that inhibits translation initiation, J. Med. Chem. 47 (2004) 4979–4982.

[31] V.R. Solomon, C. Hu, H. Lee, Design and synthesis of anti-breast cancer agents from 4-piperazinylquinoline: a hybrid pharmacophore approach, Bioorg. Med. Chem. 18 (2010) 1563–1572.

[32] R. Gudipati, R.N.R. Anreddy, S. Manda, Synthesis, anticancer and antioxidant activities of some novel *N*-(benzo[d]oxazol-2-yl)-2-(7- or 5-substituted-2-oxoindolin-3-ylidene) hydrazinecarboxamide derivatives, J. Enzyme Inhib. Med. Chem. 26 (2011) 813–818.

[33] W.-Y. Wu, S.-L. Cao, B.-B. Mao, J. Liao, Z.-F. Li, H.-B. Song, X. Xu, Synthesis and antiproliferative evaluation of hybrids of indolin-2-one and quinazoline-4(3*H*)-one linked *via* Imine bond, Lett. Drug Des. Discov. 10 (2013) 61–66.

[34] M. Sharma, S. Sharma, A. Buddhiraja, A.K. Saxena, K. Nepali, P.M.S. Bedi, Synthesis and cytotoxicity studies of 3,5-diaryl *N*-acetylpyrazoline—isatin hybrids, Med. Chem. Res. 23 (2014) 4337–4344.

[35] H.A. Abdel-Aziz, T. Elsaman, A. Al-Dhfyan, M.I. Attia, K.A. Al-Rashood, A.M. Al-Obaid, Synthesis and anticancer potential of certain novel 2-Oxo-*N*′-(2-oxoindolin-3-ylidene)-2*H*-chromene-3-carbohydrazides, Eur. J. Med. Chem. 70 (2013) 358–363.

[36] H.E. Dweedar, H. Mahrous, H.S. Ibrahim, H.A. Abdel-Aziz, Analogue-based design, synthesis and biological evaluation of 3-substituted-(methylenehydrazono)indolin-2-ones as anticancer agents, Eur. J. Med. Chem. 78 (2014) 275–280.

[37] A.S. Davari, K. Abnous, S. Mehri, M. Ghandadi, F. Hadizadeh, Synthesis and biological evaluation of novel pyridine derivatives as potential anticancer agents and phosphodiesterase-3 inhibitors, Bioorg. Chem. 57 (2014) 83–89.

[38] T. Lu, A.W. Goh, M. Yu, J. Adams, F. Lam, T. Teo, P. Li, B. Noll, L. Zhong, S. Diab, O. Chahrour, A. Hu, A.Y. Abbas, X. Liu, S. Huang, C.J. Sumby, R. Milne, C. Midgley, S. Wang, Discovery of (*E*)-3-((Styrylsulfonyl)methyl)pyridine and (*E*)-2-((Styrylsulfonyl)methyl)pyridine derivatives as anticancer agents: synthesis, Structure–Activity relationships, and biological activities, J. Med. Chem. 57 (2014) 2275–2291.

[39] M.H. Helal, S.A. El-Awdan, M.A. Salem, T.A. Abd-elaziz, Y.A. Moahamed, A.A. El-Sherif, G.A.M. Mohamed, Synthesis, biological evaluation and molecular modeling of novel series of pyridine derivatives as anticancer, anti-inflammatory and analgesic agents, Spectrochim. Acta, Part A 135 (2015) 764–773.

[40] S. Wilhelm, C. Carter, M. Lynch, T. Lowinger, J. Dumas, R.A. Smith, B. Schwartz, R. Simantov, S. Kelley, Discovery and development of sorafenib: a multikinase inhibitor for treating cancer, Nat. Rev. Drug Discov. 5 (2006) 835–844.

[41] S. DiGiulio, FDA Approves stivarga for advanced GIST, Oncol. Times 35 (2013) 12.

[42] J.J. Cui, M. Tran-Dubé, H. Shen, M. Nambu, P.-P. Kung, M. Pairish, L. Jia, J. Meng, L. Funk, I. Botrous, M.M. Tigue, N. Grodsky, K. Ryan, E. Padrique, G. Alton, S. Timofeevski, S. Yamazaki, Q. Li, H. Zou, J. Christensen, B. Mroczkowski, S. Bender, R.S. Kania, M.P. Edwards, Structure based drug design of crizotinib (PF-02341066), a potent and selective dual inhibitor of mesenchymal-epithelial transition factor (c-MET) kinase and anaplastic lymphoma kinase (ALK), J. Med. Chem. 54 (2011) 6342–6363.

[43] V. Onnis, M.T. Cocco, R. Fadda, C. Congiu, Synthesis and evaluation of anticancer activity of 2-arylamino-6-trifluoromethyl-3-(hydrazonocarbonyl)pyridines, Bioorg. Med. Chem. 17 (2009) 6158–6165.

[44] S. Zheng, Q. Zhong, M. Mottamal, Q. Zhang, C. Zhang, E. LeMelle, H. McFerrin, G. Wang, Design, synthesis, and biological evaluation of novel pyridine-bridged analogues of combretastatin-A4 as anticancer agents, J. Med. Chem. 57 (2014) 3369–3381.

[45] T. Aboul-Fadl, A. Kadi, H.A. Abdel-Aziz, Novel N,N′-Hydrazino-bis-isatin Derivatives with Selective Activity Against Multidrug-Resistant Cancer Cells. U. S. Pat., 2012, 20120252860.

[46] H.A. Abdel-Aziz, T. Aboul-Fadl, A.M. Al-Obaid, M. Ghazzali, A. Al-Dhfyan, A. Contini, Design, synthesis and pharmacophoric model building of novel substituted nicotinic acid hydrazones with potential antiproliferative activity, Arch. Pharm. Res. 35 (2012) 1543–1552.

[47] H.A. Abdel-Aziz, H.A. Ghabbour, W.M. Eldehna, M.M. Qabeel, H.-K. Fun, Synthesis, crystal structure, and biological activity of cis/trans amide rotomers of (*Z*)-*N*′-(2-Oxoindolin-3-ylidene)formohydrazide, J. Chemother. (2014) 7. Article ID 760434.

[48] A.A. Nagle, S.A. Reddy, H. Bertrand, H. Tajima, T.-M. Dang, S.-C. Wong, J.D. Hayes, G. Wells, E.-H. Chew, 3-(2-Oxoethylidene)indolin-2-one derivatives activate Nrf2 and inhibit NF-κB: potential candidates for chemoprevention, ChemMedChem (2014), http://dx.doi.org/10.1002/cmdc.201402038. Accepted manuscript.

[49] P. Skehan, R. Storeng, D. Scudiero, A. Monks, J. McMahon, D. Vistica, J.T. Warren, H. Bokesch, S. Kenney, M.R. Boyd, New colorimetric cytotoxicity assay for anticancer-drug Screening, J. Natl. Cancer Inst. 82 (1990) 1107–1112.

[50] A.K. Ghose, G.M. Crippen, Atomic physicochemical parameters for three-dimensional structure-directed quantitative structure-activity relationships I. Partition coefficients as a measure of hydrophobicity, J. Comput. Chem. 7 (1986) 565–577.

[51] B. Al-Saleh, M.M. Abdel-Khalik, A.M. Eltoukhy, M.H. Elnagdi, Enaminones in heterocyclic synthesis: a new regioselective synthesis of 2,3,6-trisubstituted pyridines, 6-Substituted-3-aroylpyridines and 1,3,5-triaroylbenzenes, J. Heterocycl. Chem. 39 (2002) 1035–1038.

[52] S.M. Agamy, M.M. Abdel-Khalik, M.H. Mohamed, M.H. Elnagdi, Enaminones as building blocks in heterocyclic synthesis: a new one pot synthesis of polyfunctional substituted pyridines, Z. Naturforsch. B 56 (2001) 1074–1078.